

## THE NASA LANGLEY ISOLATOR DYNAMICS RESEARCH LAB

T. F. Middleton\*, R. Jeffrey Balla<sup>+</sup>, R. A. Baurle\*, W. M. Humphreys<sup>+</sup>  
*NASA, Langley Research Center, Hampton, Virginia*

L. G. Wilson\*  
*Lockheed Martin, NASA, Langley Research Center, Hampton, Virginia*

### ABSTRACT

The Isolator Dynamics Research Lab (IDRL) is under construction at the NASA Langley Research Center in Hampton, Virginia. A unique test apparatus is being fabricated to support both wall and in-stream measurements for investigating the internal flow of a dual-mode scramjet isolator model. The test section is 24 inches long with a 1-inch by 2-inch cross sectional area and is supplied with unheated, dry air through a Mach 2.5 converging-diverging nozzle. The test section is being fabricated with two sets (glass and metallic) of interchangeable sidewalls to support flow visualization and laser-based measurement techniques as well as static pressure, wall temperature, and high frequency pressure measurements. During 2010, a CFD code validation experiment will be conducted in the lab in support of NASA's Fundamental Aerodynamics Program. This paper describes the mechanical design of the Isolator Dynamics Research Lab test apparatus and presents a summary of the measurement techniques planned for investigating the internal flow field of a scramjet isolator model.

### INTRODUCTION

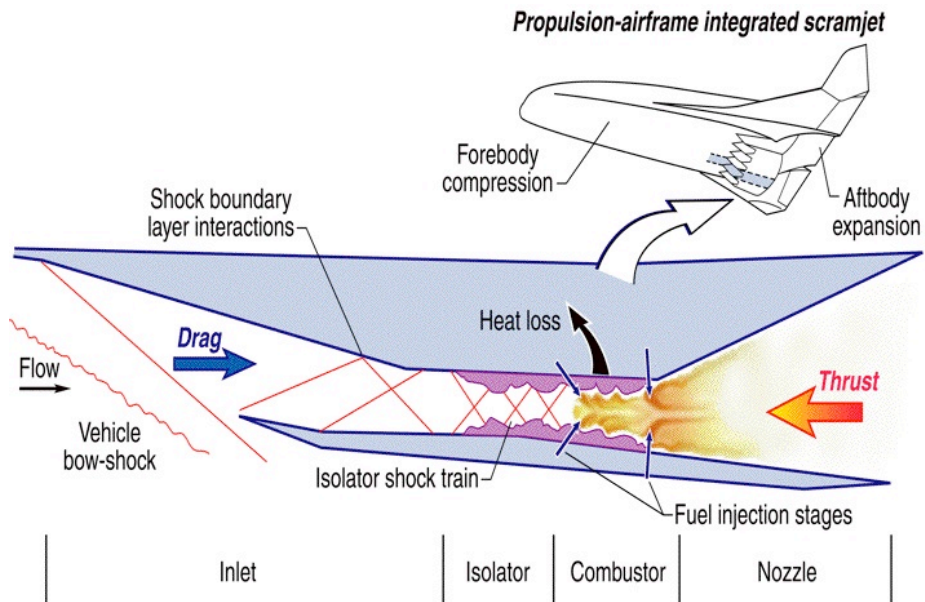
Scramjet propulsion powered hypersonic vehicles require a high degree of integration between the propulsion system and the vehicle's airframe. The forebody surface of the airframe provides a compression surface, which processes the flow passing through the vehicle bow shock. The processed flow near the forebody surface is captured by the inlet and passes into the dual-mode scramjet isolator. The primary functions of the isolator are to deliver a uniform, high-pressure flow to the combustor with minimal aerodynamic losses and to prevent the pressure waves generated in the combustor from propagating upstream into the inlet, potentially causing the inlet to unstart.<sup>1-4</sup> In the combustor, fuel is injected, mixed, and reacted with the oxygen in the high pressure flow exiting the isolator. The reacted flow expands through the scramjet nozzle and along the aftbody of the vehicle's airframe to produce thrust. Figure 1 shows the components of a typical propulsion-airframe integrated dual-mode scramjet and illustrates how the back-pressure from the combustion process causes the boundary layer in the isolator to separate and an oblique shock train to form.

In cold-flow experimental configurations, the combustor pressure rise is commonly simulated using mechanical means, such as a flow-restricting valve.<sup>5</sup> The shock pattern that develops in the isolator for a given isolator inflow condition varies as a function of the ratio of the back-pressure to the inflow static pressure.<sup>6</sup> For a high pressure ratio, the boundary layer separates and a pattern of oblique shocks form a shock train within the isolator. The complex flow field has been investigated both numerically and experimentally. However, the vast majority of the experimental measurements have been limited to wall pressure, in-stream Pitot pressure, and stagnation temperature with a limited amount of nonintrusive measurements, such as shadowgraph and spark schlieren photography.<sup>7-11</sup>

---

\* Hypersonic Airbreathing Propulsion Branch, MS-168

+ Advance Sensing and Optical Measurement Branch, MS-493



KRRLH02072001

Figure 1. Components of a typical propulsion-airframe integrated dual-mode scramjet and features of the associated internal flow.

The NASA Langley Isolator Dynamics Research Lab (IDRL) will support both wall and in-stream measurements for investigating the internal flow of a dual-mode scramjet isolator model. The 28 inch long Mach 2.5 nozzle and isolator test section assembly is supplied with unheated, dry air from an ASME Pressure Vessel Code stamped settling chamber. Two sets of interchangeable sidewalls (glass and metallic) are available to support flow visualization and laser-based measurement techniques as well as wall static pressure, temperature, and high frequency pressure measurements. Figure 2 shows the key sections that make up the test apparatus. Note, in Figure 2 the assembly is shown in a horizontal orientation for illustrative purpose. In the laboratory, the assembly will be installed vertically with a bottom-to-top flow direction.

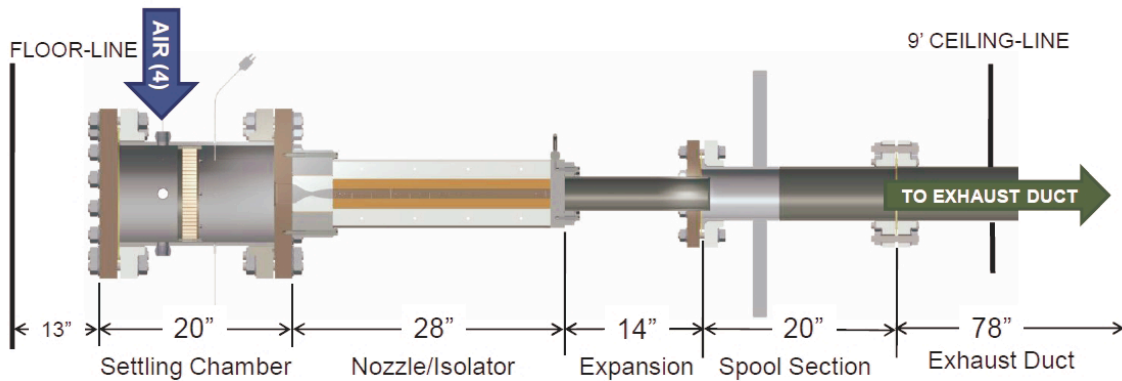


Figure 2. Assembly of the NASA Langley Isolator Dynamics Research Lab Test Apparatus.

## DESIGN OF THE IDRL TEST APPARATUS

The settling chamber function is to condition the high-pressure air and establish the total pressure for the test. High-pressure air is supplied to the settling chamber from a 1,000 psia air line reduced to 250 psia (max) within the settling chamber. The high-pressure air exits the settling chamber through the Mach 2.5 nozzle and flows through the 1-inch by 2-inch cross sectional area isolator where it adjusts to match the back-pressure condition set by the mechanical back-pressure plug. The contour of the Mach 2.5 Nozzle was determined from the Method of Characteristics (MOC) and refined by a full Navier-Stokes Solver to limit the Mach number variation across the core exit area to within 0.2% of the design Mach number.

The required isolator length was calculated using an analytical model developed at NASA Langley Research Center.<sup>2</sup> The model input parameters were obtained from a three dimensional CFD simulation using the VuLCAN full Navier-Stokes solver.<sup>12-15</sup> The required isolator length was set equal to the minimum length required to contain the shock train under a highly back-pressured condition plus two hydraulic diameters to account for uncertainty in the calculation. The isolator test section is directly connected to an expansion section with a cross-sectional area 3.5 times the isolator cross-sectional area, which is back-pressured by a position-controlled conical plug. The flow passes through the back-pressure device and enters a flexible duct leading to a muffler on the roof of the building where the flow exhausts to the atmosphere.

### Settling Chamber:

The settling chamber, shown in Figure 3, is designed in accordance with the ASME Boiler & Pressure Vessel Code for a stagnation condition of 300 psia at ambient temperature. A honeycomb flow straightener is mounted in the flow to remove any swirl and reduce the free stream turbulence level that may be present in the flow entering the settling chamber from the high-pressure air supply piping. The downstream flange is machined with a 2-inch by 2-inch opening that mates with the subsonic portion of the Mach 2.5 converging-diverging nozzle. The flow velocity in the settling chamber is limited to about 6 ft/sec to ensure the flow properties are nearly uniform entering the Mach 2.5 nozzle.

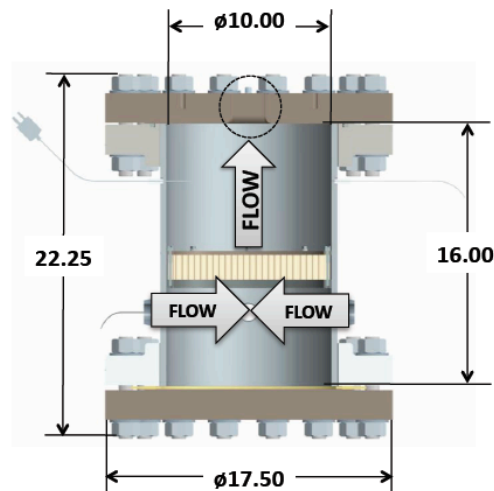


Figure 3. IDRL Settling Chamber. Dimensions are in inches.

### Mach 2.5 Converging-Diverging Nozzle:

The Mach 2.5 converging-diverging nozzle is shown in Figure 4. The contoured surfaces of the nozzle were designed as inserts that are shimmed at assembly to insure the ratio of the exit area to the nozzle throat is precisely controlled.

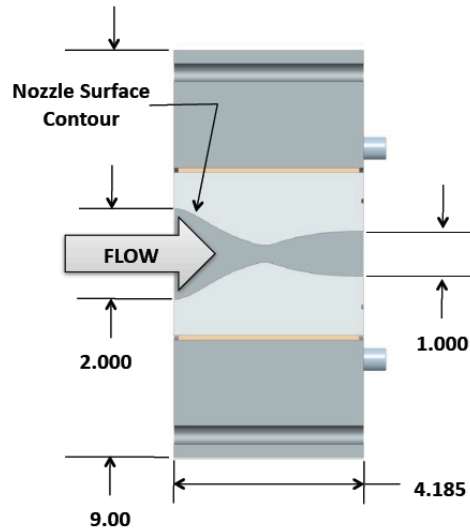


Figure 4. IDRL Mach 2.5 nozzle assembly showing contoured inserts shimmed within the nozzle block. Dimensions are in inches.

The contour for the Mach 2.5 nozzle was generated using the inviscid Method-of-Characteristics (MOC). To account for viscous effects, the nozzle flow field and the exit Mach number profile were then resolved using the Full Navier-Stokes (FNS) solver, VULCAN. Comparing the MOC solution with the FNS solution, a new exit Mach number was selected and the MOC reapplied to generate a new nozzle contour. The flow field was again resolved for the new nozzle contour using the FNS solver. This process was repeated until the percent difference in the exit core-flow Mach number profile varied by less than 0.2%. The Mach contours of the final design are shown in Figure 5. The exit Mach number and static pressure profiles from the final FNS solution are shown in Figure 6.

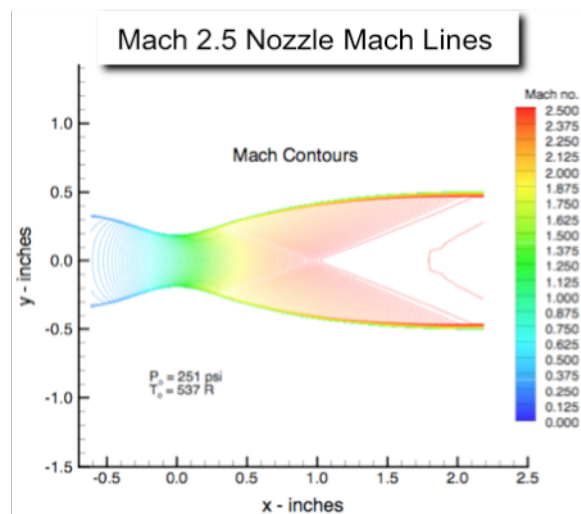


Figure 5. Mach contours for a planar Mach 2.5 nozzle designed for the IDRL test apparatus.

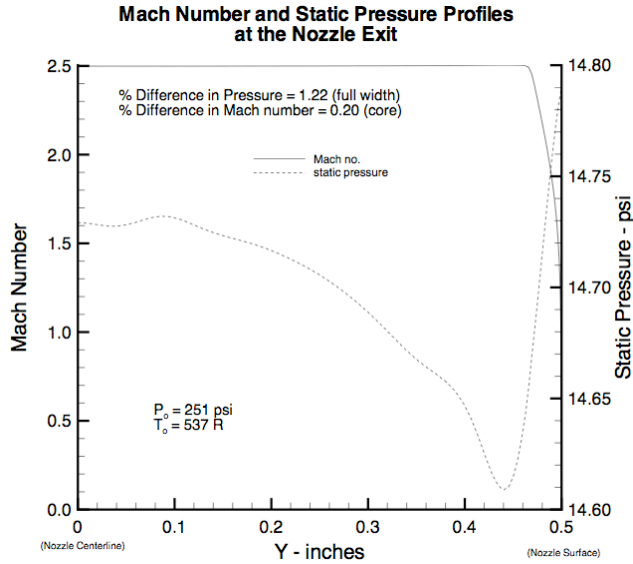


Figure 6. Mach number (left scale) and static pressure (right scale) profiles at exit of Mach 2.5 nozzle.

Isolator Test Section:

The 24-inch long test section is designed with a 1-inch by 2-inch cross sectional flow area. The sidewalls are sealed with thin gasket material and sandwiched between four strong-back supports. The strong-back supports are assembled between the Mach 2.5 nozzle flange and a corresponding downstream flange to structurally support the entire test section. Each of the sidewalls (glass and metallic) is machined identically and is interchangeable with any other sidewall. This permits mixing and matching of glass and metallic walls to obtain both wall measurements and in-stream measurements simultaneously. The assembly and cross sectional area of the test section are shown in Figures 7a and 7b, respectively.

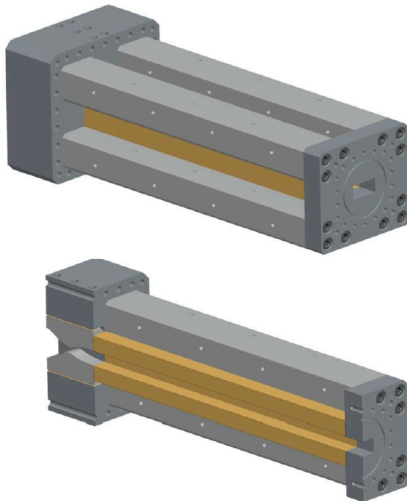


Figure 7a. IDRL isolator test section.

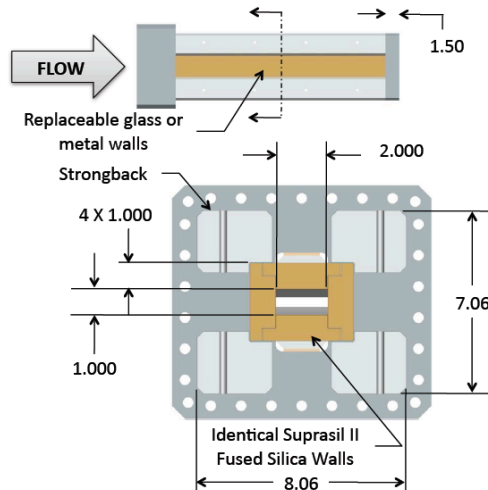


Figure 7b. Cross sectional view of test section. Dimensions are in inches.

The metallic walls are instrumented with 213 static pressure ports, 6 recovery temperature thermocouples and 16 high frequency pressure measurements ports. The various walls and the instrumentation locations are shown in Figure 8. A total of 70 static pressure ports are aligned along the centerline of the top wall with a select number mounted along each of the other sidewalls at corresponding axial locations. The pressure ports along the top wall are spaced ¼ inch apart from axial coordinate station X=0.25 to X=16. The remaining 6 ports are located 1-inch apart from X=17 to X=22. The decision to place the high concentration of pressure ports along the first 16 inches of the isolator test section was based on CFD simulations that predicted the location of the shock train under high back-pressure operation.

### IDRL Isolator Instrumentation Schematics (04-01-09)

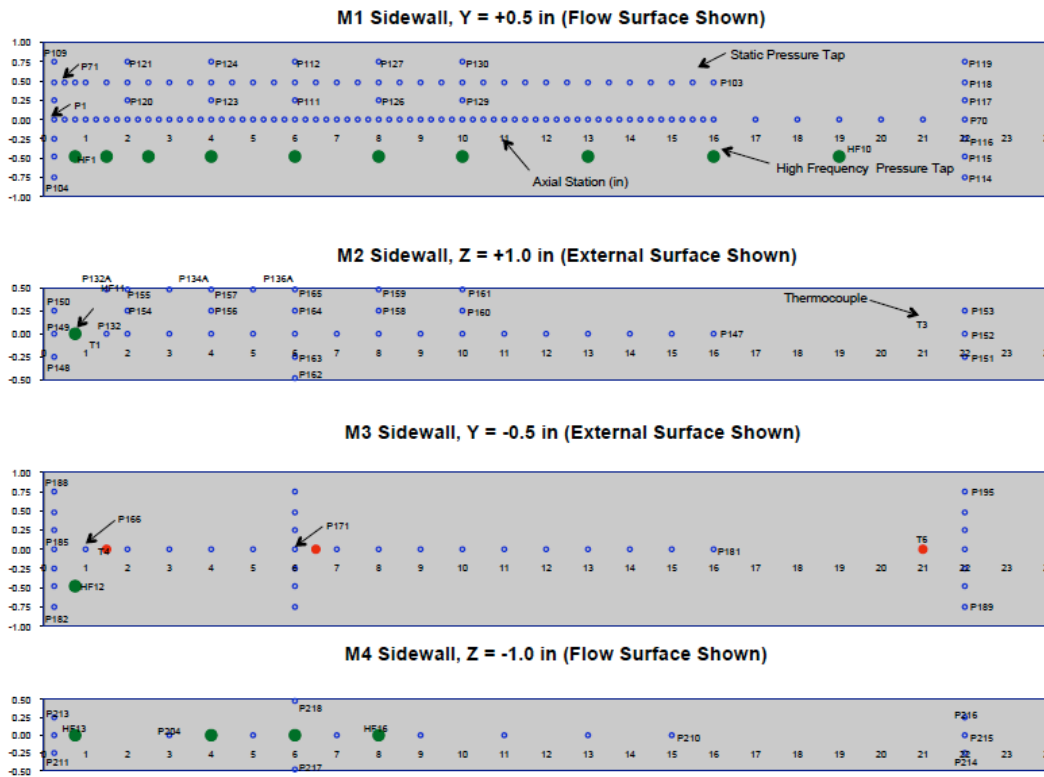


Figure 8. Instrumentation locations for metallic sidewalls of the IDRL test section. Dimensions are in inches.

The glass sidewalls, fabricated from Silica Fused Glass with 80% transmission at 180 nm, will provide full optical access when flow visualization measurement techniques are employed. As part of the CFD model validation experiment, schlieren measurements will be employed to qualitatively observe the incipient shock train and guide the research team in analyzing the quantitative data from the wall measurements and in-stream laser-based measurements.

While the rest of the IDRL test apparatus is designed for a maximum design pressure of 300 psia, the glass test section walls are limited to 77 psia to meet the safety factor of 10 required

by NASA Langley Procedural Requirements 1710.15.<sup>16</sup> Mechanical stops and redundant safety interlocks are installed to assure the internal pressure does not exceed this pressure limit when the glass walls are used.

Expansion Section, Spool Piece, and Flexible Exhaust Duct:

The flow exiting the 1-inch by 2-inch rectangular isolator section enters a 15-inch long cylindrical expansion section that is machined with a 45° chamfer on the downstream end to mate with a back-pressure plug. The back-pressure plug is mounted to a linear actuator inside a spool piece flange connected to the downstream end of the expansion section. The expansion section and spool piece are shown in Figures 9a and 9b, respectively.

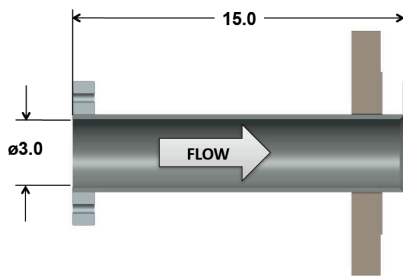


Figure 9a. Expansion Section.  
Dimensions are in inches.

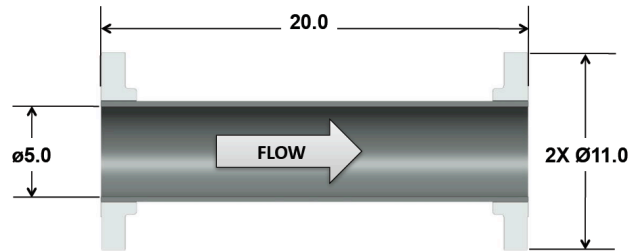


Figure 9b. Spool Piece.  
Dimensions are in inches.

The linear actuator is controlled remotely to incrementally position the back-pressure plug within the spool piece. The actuator was selected for its ability to accurately position the back-pressure plug within 1/1000 of an inch to assure repeatability of the back-pressure condition. The flow exiting the isolator passes through the expansion section, and then through the restricted cross sectional area generated by the back-pressure plug, and finally exits the facility through a flexible duct connected to a muffler system outside the building. The flexible duct, shown in Figure 10, allows for vertical movement of the entire test apparatus to permit continuous mapping of the flow field without repositioning the laser measurement system.

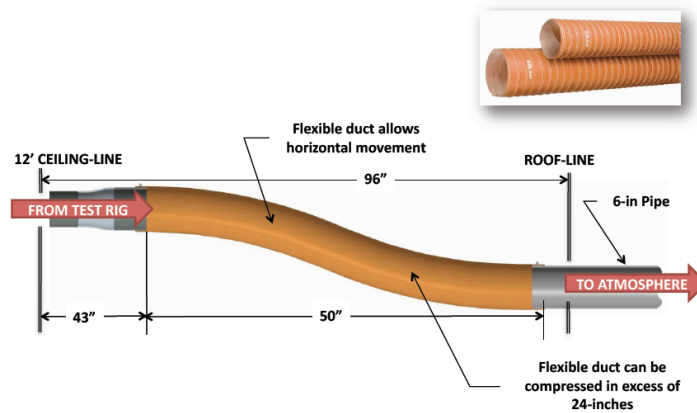


Figure 10. Flexible Exhaust Duct

## MEASUREMENT TECHNIQUES

### Design Requirements:

The IDRL was designed with the measurement techniques it will support in mind. The large number of pressure taps and surface mounted thermocouples required metallic sidewalls to maintain the structural integrity of the test section. However, to support optics- and laser-based measurements, glass sidewalls with 80% transmission at 180 nm and full optical access were required. These competing requirements were achieved by designing interchangeable sidewalls of glass and metal that could be mixed and matched. Additionally, structural members (strong-backs) were designed to support the sidewalls under internal pressure and maintain full optical access.

To support mapping of the entire flow field, the entire test apparatus was designed to translate in three dimensions. This requirement was met by mounting the entire test apparatus in a support system equipped with linear actuators capable of translating the test apparatus in three dimensions. This feature eliminates the tedious task of aligning the laser-based measurement systems for each new in-stream measurement. Additionally, the entire test apparatus can be manually rotated to permit measurements from each of the four sides of the isolator test section.

### Planned Measurements:

The primary purpose of the IDRL is to support multiple measurement techniques to measure fluid dynamic and thermodynamic properties of the flow field within a dual-mode scramjet isolator. The experimental research performed in the IDRL will be to investigate the complex fluid mechanic processes in a highly back-pressured dual-mode scramjet isolator and to provide validation data for CFD models that are employed to characterize the isolator flow field.<sup>17</sup> The selection of the experimental techniques and the development of the research plan have been coordinated with the CFD-model developer's need for accurate in-stream data.<sup>18</sup>

To characterize the complex flow within the dual-mode scramjet isolator; the recovery temperature will be measured using a thermocouple probe, the incipient shock location will be determined from wall pressure taps, and the free-stream static and stagnation pressures will be obtained from Pitot measurements near the nozzle exit. Kulite, high frequency transducers, will be placed along the top and bottom walls of the isolator to measure the high frequency pressure fluctuations and assess differences between the fluctuations along the top and bottom walls. Schlieren or shadowgraph measurements will be made to qualitatively observe the shock train formed in the isolator and will be correlated with the wall pressure measurements. Particle Imaging Velocimetry (PIV), Raman spectroscopy, and Laser Induced Thermal Acoustics (LITA)<sup>19-24</sup> measurements will be incorporated to measure the free-stream velocity and the velocity profile within the boundary layer along with temperature, density, and pressure. Table 1 outlines the measurement techniques planned for this experiment.

| Sequence | Technique   | Parameter  | Type                                   | Result  |
|----------|---|--|--|---|
| 1        | Thermocouples<br>Transducers<br>Pitot Probe<br>Kulite | Temperature<br>Wall Pressure<br>Stagnation Pressure<br>High Freq. Pressure | Point<br>Point<br>Point<br>Fluctuation | Recovery Temperature,<br>Shock Location,<br>Pitot Flow Velocity,<br>Unsteady Pressure |
| 2        | Schlieren or<br>Shadowgraph                           | Flow Visualization   | Plane                                  | Shock Location  |
| 3        | PIV   | Velocity   | Plane                                  | Free-stream Velocity  |
| 4        | Raman   | $T_{rot}$ , Density,<br>Pressure   | Point                                  | High Resolution<br>BL Measurements  |
| 5        | LITA  | Speed of Sound<br>Temperature<br>Velocity                                  | Local<br>Local<br>3 Component          | Full Mapping of Flow<br>Field,<br>Instantaneous<br>Measurements of<br>T, u, v, w      |

Table 1. Suite of measurement techniques to be employed in the IDRL.

Analysis of Lag Time Associated with PIV Seed Particles:

Recently a preliminary analysis of the lag time of PIV seed particles tracking the actual fluid flow was performed to determine the optimal size and composition for the seed particles. The lag time is aggravated by the high-speed flow and the oblique shocks within the isolator. The difference in the particle instantaneous velocity and the actual fluid velocity is computed as a function of the relative Reynolds number, the particle mass, and the particle drag coefficient. Representative results for the velocity of the fluid and the velocity of a PIV seed particle traveling along the centerline of the isolator are shown Figure 11. The results indicate that silica particles between 0.8 and 1.0 micrometers have acceptable characteristics for PIV measurements in the IDRL isolator test section. Furthermore, fabrication methods that will permit fabrication of a collection of monodisperse particles of select diameters are currently under development at NASA Langley Research Center.

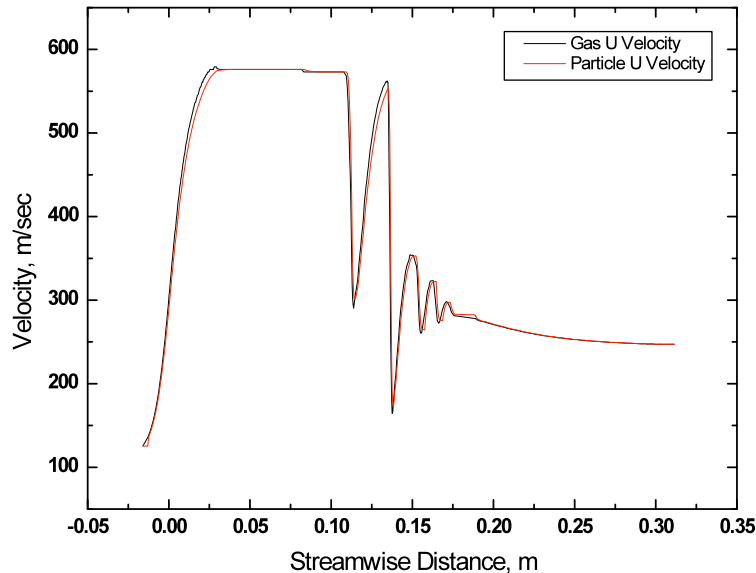


Figure 11. Representative results for PIV particle characteristics study.

### SUMMARY AND CONCLUSIONS

NASA's Fundamental Aeronautics Program has funded the construction of the Isolator Dynamics Research Lab described in this paper. The test section was uniquely designed with interchangeable (glass and metallic) sidewalls to permit both wall and in-stream measurements. The test apparatus is mounted in a support structure equipped with linear actuators capable of translating the test apparatus in three dimensions to permit a complete mapping of the flow field with a stationary optics- or laser-based measurement system. Both fluid dynamic and thermodynamic properties of the flow can be obtained simultaneously from wall and in-stream measurements. The unique design of the test apparatus coupled with the ability to perform wall and in-stream measurements simultaneously will permit a detailed mapping of the flow field for validation of CFD models.

### ACKNOWLEDGMENTS

I would like to thank the NASA research team for their enthusiasm in the planned research and especially the mechanical engineers/designers, Cyrl Jos and Joseph Alifano of ATK GASL, for their superb design capability and valuable suggestions that led to the design of such a high quality test apparatus.

### REFERENCES

1. Reintarz, B. U.; Herrmann, C. D.; Ballmann, J.: ***Aerodynamic Performance Analysis of a Hypersonic Inlet Isolator Using Computation and Experiment***. Journal of Propulsion and Power, Vol. 19, No. 5 (2003)
2. Auslender, A. H.: ***An Analytic Performance Investigation of Mechanically Back-Pressured Ramjet Data***. JANNAF 34<sup>th</sup>, October 27-31 (1997)

3. Rice, T.: **High Aspect Ratio Isolator Performance for Access-to-Space Vehicles**. AIAA 2003-7041 (2003)
4. Emami, S; Trexler, C. A.; Auslender, A. H.; Weidner, J. P.: **Experimental Investigation of Inlet-Combustor Isolators for a Dual-Mode Scramjet at a Mach Number of 4**. NASA Technical Paper 3502 (1995)
5. Hass, M; Karanian, A. J.: **Small-Scale Supersonic Inlet Test Facility**. AIAA 80-1145
6. Lin, P.; Rao, G. V. R.; O'Connor, G. M.: **Numerical Analysis of Normal Shock Train in a Constant Area Isolator**. AIAA 91-2162 (1991)
7. Waltrup, P. J.; Billig, F. S.: **Structure of Shock Waves in Cylindrical Ducts**. AIAA Vol. 11, No. 10, October (1973)
8. Sullins, G.: **Experimental Results of Shock Trains in Rectangular Ducts**. AIAA 92-5103 (1992)
9. Wang, C. P.; Zhang, K. Y.; Yang, J. J.: **Analysis of Flows in Scramjet Isolator Combined with Hypersonic Inlet**. Presented at AIAA meeting, January 10-13, 2005, Reno Nevada (2005)
10. Carroll, B. F.; Dutton, J. C.: **Characteristics of Multiple Shock Wave/Turbulent Boundary-Layer Interactions in Rectangular Ducts**. J. Propulsion, Vol. 6, No. 2 (1990)
11. Kumar, A.; Balu, G.; Panneerselvam, S.; Rathakrishnan, E.: **Performance of an Isolator Fed with Parallel Flow**. Presented at AIAA meeting, July 10-13, 2005, Tucson, Arizona (2005)
12. Baurle, R. A. (web site Curator): <http://vulcan-cfd.larc.nasa.gov>
13. Edwards, J. R.: **A Low Diffusion Flux-Splitting Scheme for Navier-Stokes Calculations**. Computers and Fluids, Vol. 26, No. 6, 635-659 (1997)
14. Wilcox, D. C.: **Turbulence Modeling for CFD**. DCW Industries, Inc. Edition 2<sup>nd</sup>, (1998)
15. Wilcox, D. C.: **Wall Matching, a Rational Alternative to Wall Functions**. AIAA 89-0611, January (1989)
16. Freeman, D. C. Jr., **LPR 1710.15, WIND-TUNNEL MODEL SYSTEMS CRITERIA** (22 JUL 2004)
17. Middleton, T. F.; Balla, R. Jeffrey; Baurle, R. A.; Wilson, L. G.: **Laser Induced Thermal Acoustic Measurements in a Highly Back-Pressured Scramjet Isolator Model: A Research Plan**. JANNAF 30<sup>th</sup> Airbreathing Propulsion May 12-16 (2008)
18. Gaffney, R. L. Jr.; Cutler, A. D.: **CFD Modeling Needs and What Makes a Good Supersonic Combustion Validation Experiment**. Presented at the JANNAF Conference, Charleston, SC, June (2005)
19. Hart, R. C.; Balla, R. J.; Herring, G. C.: **Non-resonant Referenced LITA Thermometry in Air**. Applied Optics, 38, 577-584 (1999)
20. Hart, R. C.; Balla, R. J.; Herring, G. C.: **Optical Measurement of the Speed-of-Sound in Air Over the Temperature Range 300-650K**. The Journal of Acoustical Society of America, 108, 1946-1948 (2000)
21. Hart, R. C.; Balla, R. J.; Herring, G. C.: **Simultaneous Velocimetry and Thermometry of Air by Use of Nonresonant Heterodyned Laser-Induced Thermal Acoustics**. Applied Optics, 40, 965-968 (2001)
22. Eckbreth, A. C.: **Laser Diagnostics for Combustion and Species**, Volume 7, Energy and Engineering Science Series: Abacus Press, (1988)
23. Cummings, E. B.: **Laser Induced Thermal Acoustics**. PhD Thesis, California Institute of Technology, Pasadena, California (1995)
24. Stampanoni-Panariello, A.; Hemmerling, B.; Hubschmid, W.: **Temperature Measurements in gases using laser-induced electrostrictive gratings**. Springer-Verlag: Applied Physics B, Laser and Optics (1998)